



1 Differential photosynthetic response of marine planktonic and
2 benthic diatoms to ultraviolet radiation under various temperature
3 regimes

4 Yaping Wu¹, Furong Yue², Juntian Xu^{2,*}, John Beardall³

5 1. College of Oceanography, Hohai University, Nanjing, 210098, China

6 2. College of Marine Life and Fisheries, Huaihai Institute of Technology, Lianyungang,
7 222005, China

8 3. School of Biological Sciences, Monash University, Clayton, Victoria 3800, Australia

9

10

11 * Author correspondence: jtxu@hhit.edu.cn



12 **Abstract:**

13 We studied the photophysiological response to ultraviolet radiation (UVR) of two
14 diatoms, isolated from different environmental niches. Both species showed the highest
15 sensitivity to UV radiation under relatively low temperature, while they were less
16 inhibited under moderately increased temperature. Under the highest temperature
17 applied in this study, the benthic diatom *Nitzschia sp.* showed minimal sensitivity to
18 UV radiation, while inhibition of the planktonic species, *Skeletonema sp.*, increased
19 further compared with that at the growth temperature. These photochemical responses
20 were linked to values for the repair and damage processes within the cell; higher
21 damage rates and lower repair rates were observed for *Skeletonema sp.* under
22 suboptimal temperature, while for *Nitzschia sp.*, repair rates increased and damage rates
23 were stable within the applied temperature range. Our results suggested that the
24 response of phytoplankton to UV radiation correlated with their niche environments,
25 the periodic exposure to extreme temperature promote the resistance of benthic species
26 to the combination of high temperature and UV radiation. Furthermore, the
27 temperature-mediated UV sensitivities might also have implications for phytoplankton
28 in the future warming oceans.

29 **Keywords:** Diatom, Photosynthetic performance, Temperature, UV radiation

30

31

32

33

34



35 **Introduction**

36 As the most abundant group of phytoplankton, and one that plays an important
37 role in marine ecosystem function and biogeochemical cycles, diatoms are traditionally
38 divided into centric and pennate species on the basis of their valve symmetry (Round
39 et al., 1990). Centric diatoms are usually, though not invariably, planktonic and pennate
40 species are benthic, and are often found living in different niches (Irwin et al.,
41 2012; Keithan et al., 1988). The distribution of centric diatoms is more widespread, with
42 records for the open ocean as well as coastal water, and they maintain position in the
43 upper mixing layer by maintaining buoyancy with elaborated spines or excretion of
44 heavy ions (Lavoie et al., 2016; Villareal, 1988). In contrast, pennate diatoms are often
45 found in the intertidal zone (Stevenson, 1983). Therefore, the 2 groups of diatom are
46 likely to have evolved different strategies to cope with their niche environments
47 (Barnett et al., 2015; Lavaud et al., 2016; Lavaud et al., 2007).

48 Temperature affects almost all biochemical reactions in living cells, and is one of
49 the most important factors that determines the biogeography, as well as the temporal
50 variation of phytoplankton (Levasseur et al., 1984). Under global change scenarios,
51 increases in sea surface temperature would re-structure the phytoplankton assemblages
52 in the future ocean (Thomas et al., 2012). At small spatial scales, e.g. the coastal zone,
53 diurnal cycle of tides or meteorological events could expose benthic diatoms to extreme
54 environments, including high PAR and UV exposure as well as larger variations in
55 temperature than found for planktonic species. Hence organisms in such exposed areas
56 should potentially possess highly efficient mechanisms to adapt such environment
57 (Souffreau et al., 2010; Weisse et al., 2016).

58 In the intertidal zone, UV radiation (UVR) is another driving force. UVR is a
59 component of the solar spectrum, along with photosynthetically active radiation (PAR),
60 and has wide reaching effects on organisms, especially photoautotrophs due to their
61 demands for light energy (Williamson et al., 2014). The penetration of effective UVR
62 in coastal waters is mainly dependent on the properties of the seawater (Tedetti and
63 Sempere, 2006). Previous studies have found that UVR significantly inhibited carbon



64 fixation by phytoplankton in the surface layer, with less inhibition or even stimulation
65 in deep water due to low UVR and limiting levels of PAR (Gao et al., 2007).
66 Detrimental effects, however, varied seasonally, with less inhibition observed for
67 planktonic assemblages during summer, though UV radiation was the highest. This may
68 be attributable to the higher water temperature which facilitated enzyme-catalyzed
69 repair processes within the cell (Wu et al., 2010). There are few documented studies on
70 benthic species, which actually are potentially more resistant to UVR as they are
71 periodically exposed to high solar radiation during low tide (Barnett et al., 2015).

72 Photosystem II (PSII) initiates the first step of photosynthesis, converting photons
73 to electrons efficiently, but this complex is very sensitive to light (Campbell and
74 Tyystjarvi, 2012). The subunits of PSII are broken down under UVR or high PAR while
75 repaired by insertion of de-novo synthesized protein (Aro et al., 1993); the repair
76 process eventually reaches a dynamic balance with damage (Heraud and Beardall,
77 2000). However, these two processes are independent from each other. The
78 photochemical damage is mainly determined by the intensity and spectrum of light
79 (Heraud and Beardall, 2000) and is temperature insensitive, while the repair process is
80 driven by a series of enzyme-catalyzed reactions, and is thus potentially sensitive to
81 temperature changes (Melis, 1999). Previous studies revealed that high temperature
82 alleviated UV inhibition of photosystem II in green algae (Wong et al., 2015), while it
83 interactively decreased photosynthetic activity in microphytobenthos under excessive
84 PAR conditions (Laviale et al., 2015).

85 Coastal water is a highly productive zone, with most of primary productivity
86 attributed to diatoms (Carstensen et al., 2015). Hence, how diatoms respond to
87 environmental factors, e.g. UV radiation, nutrient pulses or temperature, has been
88 extensively studied (Häder et al., 2011). These responses were often shown to be
89 species-specific, and could correlate with cell size, geometry or distinct mechanisms
90 operated by different species (Halac et al., 2014; Wu et al., 2015). Considering the
91 niches in which diatoms are living, physical and chemical factors are quite different
92 between planktonic and benthic species (Souffreau et al., 2010). In this study, we will



93 use two isolated species to test the hypothesis that benthic diatoms have a stronger
94 ability to adapt to potentially stressful solar UV radiation under high temperature
95 regimes.

96 **Materials and methods**

97 1. Species and culture conditions

98 We collected samples from offshore water and intertidal sediments in the coastal
99 area of the Yellow Sea. These were re-suspended in seawater, and enriched with Aquil
100 medium and incubated in a growth chamber for 3 days (Morel et al., 1979). Then a sub-
101 sample was examined under a microscope, and single cells were picked up with a micro
102 pipette. *Skeletonema sp.* and *Nitzschia sp.* were chosen for the present study, and were
103 maintained in Aquil medium in a growth chamber at 15 °C. Prior to the experiment,
104 both species were inoculated into enriched seawater and cultured semi-continuously in
105 500 mL polycarbonate bottles, illuminated with cool fluorescent tubes at a photon flux
106 density of $\sim 200 \mu\text{mol m}^{-2} \text{s}^{-1}$, with a 12:12 light/dark cycle. While temperature was set
107 at 15, 20 or 25 °C with variation less than 0.5 °C, and culture bottles (triplicates for each
108 temperature) were manually shaken 2–3 times during light period and randomly
109 distributed in the growth chamber.

110 2. Determination of spectra and growth rate

111 50 mL of culture was filtered onto a GF/F filter, and extracted in 5 mL absolute
112 methanol for 2 h at room temperature in a 10 mL centrifuging tube, then centrifuged at
113 4000 rpm for 15 min (TDZ4-WS, Luxiang Inc.). The supernatant was scanned with a
114 spectrophotometer (Lambda 35, PerkinElmer) in the range of 280nm-750 nm. The cut-
115 off filters were scanned in the same wavelength range against air as a blank. Specific
116 growth rate was estimated from the changes of dark adapted chlorophyll fluorescence,
117 and calculated as: $\mu = (\text{Ln } F_2 - \text{Ln } F_1) / (T_2 - T_1)$, where F_1 and F_2 represent the steady-
118 state fluorescence intensity at T_1 or T_2 , respectively.

119 3. Experimental set up

120 The experiments were performed under a customized solar simulator with a 1,000
121 W xenon arc lamp as the light source. The incident irradiances of UV-B light (280–315



122 nm), UV-A (315–400 nm), and PAR (400–700 nm) were measured using a broadband
123 radiometer (SOLAR-2UV, TINEL Inc.).

124 In the middle of the light period, samples of both species in the exponential phase
125 were harvested and directly transferred to quartz tubes (35 mL) at a density of less than
126 $20 \mu\text{g chl } a \text{ L}^{-1}$, dark-adapted for 15 min, and milli-Q water (as a control) or lincomycin
127 (final concentration, 0.5 mg mL^{-1} , for the determination of damage rate in the absence
128 of repair) were added. The tubes were then placed into a water bath one after another at
129 1 minute intervals while covered with cut-off filters (ZJB280, ZJB400) that block
130 radiation below 280 or 400 nm, respectively (50% transmission at 280 nm or 400 nm,
131 see Figure A1), to create PAR + UV-A + UV-B (PAB) and PAR (P) treatments
132 respectively. The light levels applied were $\text{PAR} = 440 \mu\text{mol photons m}^{-2} \text{ s}^{-1}$ and $\text{UVR} =$
133 41.6 W m^{-2} , while temperature was controlled with a cooling system (CTP3000, Eyela)
134 and was set as the incubation level (termed “acclimated”) or incubation temperature
135 $+10 \text{ }^\circ\text{C}$ (termed “short term”), the latter mimicking a moderate increase in temperature
136 in the intertidal zone during a low tide period. After the light exposure, samples were
137 moved into a water bath at the same temperature as light exposure, but under dim light
138 ($\sim 30 \mu\text{mol photons m}^{-2} \text{ s}^{-1}$), for recovery, effective quantum yields were then measured
139 at 12 min intervals.

140 4. Chlorophyll fluorescence measurements

141 A total of 12 tubes (2 species and 2 radiation treatments) were dark-adapted for 15
142 min, then each tube was moved into water bath one by one with 1 minute interval for
143 light exposure, and sub-samples were taken to measure the initial chlorophyll
144 fluorescence with an Aquapen fluorometer (AP-C 100, PSI). During the subsequent
145 light exposure, sub-samples were withdrawn every 12 minutes from the quartz tubes
146 for fluorescence measurement, this procedure ensured that every sample was exposed
147 to radiation with exact the same time duration. After five rounds of measurements (60
148 min), samples that were without lincomycin were transferred into the low light
149 condition under the same temperature for recovery, and chlorophyll fluorescence was
150 measured as above for 60 min.



151 5. Data analysis

152 Effective quantum yields were measured with the AquaPen and calculated
 153 according to the following equations:

$$154 \quad \text{Effective quantum yield} = (F_m' - F_t) / F_m'$$

155 where F_m' is the effective maximal fluorescence, and F_t is the steady-state fluorescence
 156 under actinic light.

157 The relative inhibition of effective quantum yield by UV was estimated according
 158 to the following equation:

$$159 \quad \text{Relative inhibition (\%)} = (P_P - P_{PAB}) / P_P \times 100,$$

160 where P_P and P_{PAB} represent the effective quantum yield under P and PAB treatments,
 161 respectively. Relative inhibition was calculated when P_P and P_{PAB} were significantly
 162 different.

163 The rates of UVR-induced damage to photosystem II (PSII) (k , min^{-1}) were
 164 calculated from lincomycin treated samples assuming repair (r) under these conditions
 165 was zero. Repair rates (r , min^{-1}) were calculated using non-lincomycin-treated
 166 samples with the fixed k values obtained from the parallel experiments with lincomycin.
 167 Both calculation were according to the Kok equation (Heraud and Beardall, 2000):

$$168 \quad \frac{P_t}{P_0} = \frac{r}{k+r} + \frac{k}{k+r} e^{-(k+r)t},$$

169 where P_0 and P_t represent the initial effective quantum yield and yield at time zero
 170 and t (minutes), respectively.

171 The recovery rates under dim light were calculated with a simple exponential rise
 172 equation (Heraud and Beardall, 2000) :

$$173 \quad y = y_0 + c (1 - e^{-\alpha t})$$

174 where y represents the effective quantum yield at time t (minutes) during the dim
 175 light incubation, α was the recovery rate, while y_0 and c are constants.

176 Statistical differences among treatments were analyzed with a one-way analysis of
 177 variance (ANOVA) and Tukey HSD was conducted for *post hoc* investigation. A
 178 confidence interval of 95% was set for all tests.



179

180 **Results**

181 *Skeletonema sp.* had a lower growth rate under 15 and 20 °C ($p < 0.05$), while
182 growth increased significantly and was 23% higher than that of *Nitzschia sp.* under
183 25 °C (Fig 1) ($p < 0.01$). The spectra of methanol extracts of both species had a similar
184 pattern, *Nitzschia sp.* showed relatively higher absorption in the range of 410-480 nm
185 under 15 or 20 °C (Fig 2 A, B), and this further increased significantly under 25 °C (Fig
186 2C). While no obvious peak in the UV range for both species.

187 The initial photochemical quantum yield of 15 °C grown *Skeletonema sp.* was
188 around 0.50 during light exposure (incubated under 15 °C), but decreased gradually
189 toward the end of the radiation treatments, with lower values under PAB than the P
190 condition (Fig 3A). During the dim light exposure period, the quantum yield recovered
191 to its initial value within 24 min under P treatment, while PAB treated cells only
192 recovered partially to ~70% by the end of the dim light incubation (Fig 3A). For 15 °C
193 grown cells that were incubated under 25 °C, the general patterns were similar as under
194 15 °C, though with smaller differences between the P and PAB treatments (Fig 3B).
195 Under dim light, quantum yield of both radiation treatments recovered to near initial
196 values (Fig 3B). For 15 °C grown *Nitzschia sp.* that was measured at 15 °C, the
197 decreasing pattern under P or PAB was similar to that of *Skeletonema sp.*, while for
198 PAB exposed cells, *Nitzschia sp.* could only recover to ~50% of initial value under dim
199 light (Fig 3C). However, when 15 °C grown *Nitzschia sp.* were incubated at 25 °C for
200 light exposure, both P and PAB treated cells had higher quantum yields, with less UVR
201 suppression of photosystem II compared with 15 °C, and PAB exposed cells could
202 recover to 75% of the initial value when subsequently incubated under dim light (Fig
203 3D).

204 The 20 °C grown *Skeletonema sp.*, independent of incubation temperatures (20 or
205 30 °C), showed insignificant UV inhibition for most of time points during radiation
206 exposure, and recovered more quickly under dim light, especially for PAB treated cells
207 compared with samples under 15 °C (Fig 4 A, B). For *Nitzschia sp.* that were grown at



208 20 °C, cells showed moderate UV inhibition during radiation exposure, and the
209 quantum yield under PAB treatment only recovered to ~80% at the end of the dim light
210 incubation at 20 °C, while quantum yield recovered to the initial value in cells measured
211 under 30 °C (Fig 4 C, D).

212 *Skeletonema sp.* that was grown and measured at 25 °C showed a similar pattern
213 to that grown under 20 °C during both radiation exposure and subsequent dim light (Fig
214 5A). However, quantum yields decreased significantly once cells were moved into
215 35 °C, with much lower values observed under PAB and P treatment ($p < 0.001$) than
216 under 25 °C. During the dim light period, *Skeletonema sp.* only recovered to ~30% for
217 P treatment, while there was no recovery after the PAB treatment (Fig 5B). For
218 *Nitzschia sp.* measured under 25 or 35 °C, both treatments showed a similar response,
219 with lower values under PAB than P during the radiation exposure ($p < 0.001$ at 25 °C,
220 $p < 0.01$ at 35 °C), while cells could recover to near initial values at the end of the dim
221 light incubation (Fig 5 C, D).

222 In the presence of lincomycin, changes in effective quantum yield showed a
223 similar pattern for most of treatments (Figure A2-4), except for *Skeletonema sp.*
224 incubated under 35 °C, which had relatively lower values compared with samples under
225 25 °C (Figure A4).

226 The relative inhibition induced by UV radiation at the end of radiation exposure is
227 shown in Fig 6. Both species had the greatest sensitivities under 15 °C, with 80% and
228 70% relative inhibition of photochemical quantum yield for *Skeletonema sp.* and
229 *Nitzschia sp.*, respectively. In the range of acclimated temperature, relative UV
230 inhibition decreasing with increase of temperature for both species. While in the range
231 of short term incubation with a 10 °C increase, UV inhibition of *Skeletonema sp.* was
232 comparable at 25 °C and 30 °C, but increased significantly to ~50% at 35 °C ($p < 0.01$).
233 For *Nitzschia sp.*, relative UV inhibition during short term incubation reached a plateau,
234 in the range of 25 – 35 °C, of around 25%.

235 During radiation exposure, the repair rates for photosystem II in *Skeletonema sp.*
236 varied among different temperatures, with highest values observed at 25 °C, and lowest



237 values at 35 °C for both radiation treatments (Fig 7A). The damage rates gradually
238 decreased from 15 to 25 °C, then increased significantly toward 35 °C (Fig 7B)
239 ($p < 0.001$). The ratio of repair rate to damage rate ($r : k$) showed a unimodal pattern with
240 peak values at 25 °C, and with lowest values under 15 or 35 °C, especially for the PAB
241 treatment (Fig 7C).

242 The repair rate during light exposure for *Nitzschia sp.*, increased significantly in
243 the temperature range of 15 to 25 °C ($p < 0.001$), while kept relatively stable from 25 to
244 35 °C (Fig 8A). The damage rates were quite stable for all temperatures tested, whether
245 cells were acclimated or exposed to short term elevation of temperature, with mean
246 values around 0.075 for PAB and 0.032 for P treatment (Fig 8B). The $r : k$ ratio
247 increased with temperature in the range of 15-25 °C, reaching relatively stable values
248 of around 1.50 for PAR, and around 1.0 for the PAB treatment (Fig 8C).

249 Under dim light, the rate constant for recovery of PAR-exposed *Skeletonema sp.*
250 were around 0.10-0.15 min^{-1} in the range of 15-30 °C, while increased significantly to
251 around 0.30 at 35 °C ($p < 0.01$) (Fig 9A). The rate constant for recovery of P exposed
252 *Nitzschia sp.* was relatively stable, around 0.25 min^{-1} , in the range of applied
253 temperature (Fig 9B). The rate constant for recovery of PAB exposed *Skeletonema sp.*
254 showed an increasing pattern from 0.05 to 0.17 min^{-1} in the range of 15-25 °C, but
255 decreased significantly at 30 °C ($p < 0.05$); at 35° values were unable to be estimated
256 due to poor fitting of data points (Fig 9C). No consistent trend was found for the rate
257 constant for recovery of PAB exposed *Nitzschia sp.*, around 0.10-0.15 min^{-1} , in the
258 range of applied temperature (Fig 9D).

259 Discussion

260 The natural variation of physical and chemical factors, including nutrients, salinity,
261 temperature, light etc., provide major controls that determine the distribution,
262 succession and composition of phytoplankton (Levasseur et al., 1984). In response to
263 these variables, phytoplankton have evolved different strategies of acclimation or
264 adaptation (Irwin et al., 2015; Padfield et al., 2016). In this study, we found that both
265 benthic and planktonic diatoms were less inhibited by UVR under moderately increased



266 temperature, while the benthic species was more resistant to UVR under the extreme
267 temperature. These findings imply that temperature is a key factor that mediates the
268 response of diatoms to UVR, while different species have developed distinct
269 mechanisms in response to their particular niche environments (Laviale et al., 2015).

270 As a basic environmental factor, temperature affects all metabolic pathways, and
271 extreme or sub-optimal conditions are often encountered by various organisms in nature
272 (Mosby and Smith, 2015). The growth response of phytoplankton to temperature varies
273 from species to species, but often shows a unimodal pattern (Brown et al., 2004; Chen,
274 2015). For the applied temperature range in the present study, the growth rate of benthic
275 species showed a slight response, while growth increased with temperature to a greater
276 extent in the planktonic species, particularly above 25 °C. However, life forms in the
277 natural environment are affected by multiple stressors concomitantly (Boyd et al., 2015).
278 For instance, a recent studies have demonstrated that increased temperature would
279 interactively affect phytoplankton with light intensity (Edwards et al., 2016), and could
280 alleviate UV direct inhibition on some sensitive species (Halac et al., 2014). When
281 species were acclimated under sub-optimal temperature (15 °C), both showed obvious
282 sensitivity to UVR (Fig 3). During the recovery period, the effective quantum yield of
283 the benthic diatom could rapidly reach the highest values within 12 min irrespective of
284 the incubation temperature. The planktonic diatom, however, only performed better
285 under short term elevated temperature. This suggests that the benthic species could have
286 broader adaptability in cope with the highly varied temperature environment they
287 frequently experience (Laviale et al., 2015).

288 The operation of Photosystem II is sensitive to light intensity as well as quality.
289 High P and UVR can usually induce significant damage to this complex, while the de
290 novo synthesis of protein can replace the damaged subunit (Aro et al., 1993; Lavaud et
291 al., 2016). The damage rate (k), which represents the efficiency of detrimental effects,
292 showed a different response for the 2 species in this study; in the planktonic species, k
293 was sensitive to temperature change with the lowest value at the medium temperature,
294 but was quite stable in the benthic species at all temperatures tested. This could be



295 attributed to a decrease in electron transport, or changes in ultra-structure which
296 resulted in higher intracellular light exposure for planktonic species (Melis, 1999;Nitta
297 et al., 2005). The repair rates (r) and the ratio of r to k further demonstrated that the
298 planktonic species had a relatively lower optimal temperature in response to UVR, with
299 the highest $r:k$ and lowest UV inhibition at 25 °C. In contrast, in the benthic species r
300 and $r:k$ increased steadily and reached relatively stable values at the highest temperature,
301 and this coincided with lower UV inhibition, implying that although acclimated in lab
302 condition for weeks, this species still had an active mechanism to respond to high
303 temperature and UVR, as might occur in its natural niche environment (Laviale et al.,
304 2015).

305 In addition to repair process that are initiated after damage, UV absorbing
306 compounds could directly screen out part of the detrimental radiation, protecting
307 cellular organelles from UV damage (Garcia-Pichel and Castenholz, 1993). In diatoms,
308 however, the spectra of methanol extracts showed only a small absorbance peak in the
309 UVR. Unlike xanthophyll cycle related pigments, UV-absorbing compounds (UVAC)
310 are inducible and only synthesized under long-term UV exposure, indicating that UVAC
311 are not a major protecting mechanism for lab cultured diatoms (Helbling et al., 1996).
312 However, the xanthophyll cycle could respond quickly under photo-inhibition, and has
313 been shown to be a major mechanism in diatoms in response to high light or UV
314 (Cartaxana et al., 2013;Zudaire and Roy, 2001). Therefore, the relatively higher
315 absorption in the blue range for benthic species, might indicate that temperature
316 enhances the synthesis of xanthophyll related pigments (Havaux and Tardy, 1996).

317 The temperature dependent response to UVR has major implications for
318 phytoplankton. With the continuing emission of greenhouse gases, the surface seawater
319 temperature is predicted to increase by up to 4 °C by the end of this century (New et al.,
320 2011), and this could potentially re-shape the phytoplankton assemblages (Thomas et
321 al., 2012). While the situation might be more complex in the natural environment with
322 the consideration of interaction of UVR with other factors (Beardall et al., 2009), for
323 unicellular green algae, an increase of temperature could mitigate UVR harm for



324 temperate species, while exacerbating UV inhibition for polar species (Wong et al.,
325 2015). Moreover, the tolerance of phytoplankton to extreme temperature would be
326 latitude dependent; for tropical areas where the temperature is already high, an increase
327 of temperature reduced the richness of phytoplankton (Thomas et al., 2012).

328 The present study showed a differential response to UV radiation for two diatoms
329 from contrasting niches. As predicted, the benthic species had a higher tolerance to the
330 combination of extreme temperature and UV radiation, which can be attributed to the
331 environment in which were living. Below the optimal temperature, both species
332 performed better in response to UV radiation under elevated temperature, suggesting
333 that the natural variation of temperature due to changes in the heat flux from the sun or
334 meteorological events would alter the extent of UV effects on primary producers, and
335 therefore the aquatic ecosystem (Häder et al., 2011). Furthermore, considering the
336 projected global warming scenarios, UV radiation could impose different impacts on
337 phytoplankton with respect to the regional differences (Beardall et al., 2009; Xie et al.,
338 2010).

339 *Acknowledgement:* This study was supported by National Natural Science
340 Foundation of China (41476097) and the Fundamental Research Funds for the Central
341 Universities (2016B12814).

342


 343 **References:**

- 344 Aro, E. M., Virgin, I., and Andersson, B.: Photoinhibition of Photosystem II. Inactivation, protein
 345 damage and turnover, *Biochimica et biophysica acta*, 1143, 113-134, 10.1016/0005-2728(93)90134-
 346 2, 1993.
- 347 Barnett, A., Meleder, V., Blommaert, L., Lepetit, B., Gaudin, P., Vyverman, W., Sabbe, K., Dupuy,
 348 C., and Lavaud, J.: Growth form defines physiological photoprotective capacity in intertidal benthic
 349 diatoms, *Isme Journal*, 9, 32-45, 10.1038/ismej.2014.105, 2015.
- 350 Beardall, J., Sobrino, C., and Stojkovic, S.: Interactions between the impacts of ultraviolet radiation,
 351 elevated CO₂, and nutrient limitation on marine primary producers, *Photochemical &*
 352 *Photobiological Sciences*, 8, 1257-1265, 10.1039/b9pp00034h, 2009.
- 353 Boyd, P. W., Lennartz, S. T., Glover, D. M., and Doney, S. C.: Biological ramifications of climate-
 354 change-mediated oceanic multi-stressors, *Nature Climate Change*, 5, 71-79, 10.1038/nclimate2441,
 355 2015.
- 356 Brown, J. H., Gillooly, J. F., Allen, A. P., Savage, V. M., and West, G. B.: Toward a metabolic theory
 357 of ecology, *Ecology*, 85, 1771-1789, 10.1890/03-9000, 2004.
- 358 Campbell, D. A., and Tyystjarvi, E.: Parameterization of photosystem II photoinactivation and repair,
 359 *Biochimica Et Biophysica Acta-Bioenergetics*, 1817, 258-265, 10.1016/j.bbabbio.2011.04.010, 2012.
- 360 Carstensen, J., Klais, R., and Cloern, J. E.: Phytoplankton blooms in estuarine and coastal waters:
 361 Seasonal patterns and key species, *Estuarine Coastal and Shelf Science*, 162, 98-109,
 362 10.1016/j.ecss.2015.05.005, 2015.
- 363 Cartaxana, P., Domingues, N., Cruz, S., Jesus, B., Laviale, M., Serodio, J., and da Silva, J. M.:
 364 Photoinhibition in benthic diatom assemblages under light stress, *Aquatic Microbial Ecology*, 70,
 365 87-92, 10.3354/ame01648, 2013.
- 366 Chen, B.: Patterns of thermal limits of phytoplankton, *Journal of Plankton Research*, 37, 285-292,
 367 10.1093/plankt/fbv009, 2015.
- 368 Edwards, K. F., Thomas, M. K., Klausmeier, C. A., and Litchman, E.: Phytoplankton growth and
 369 the interaction of light and temperature: A synthesis at the species and community level, *Limnology*
 370 *and Oceanography*, 61, 1232-1244, 10.1002/lno.10282, 2016.
- 371 Gao, K., Wu, Y., Li, G., Wu, H., Villafane, V. E., and Helbling, E. W.: Solar UV radiation drives
 372 CO₂ fixation in marine phytoplankton: A double-edged sword, *Plant Physiology*, 144, 54-59,
 373 10.1104/pp.107.098491, 2007.
- 374 Garcia-Pichel, F., and Castenholz, R. W.: Occurrence of UV-Absorbing, Mycosporine-Like
 375 Compounds among Cyanobacterial Isolates and an Estimate of Their Screening Capacity, *Applied*
 376 *and environmental microbiology*, 59, 163-169, 1993.
- 377 Häder, D.-P., Helbling, E., Williamson, C., and Worrest, R.: Effects of UV radiation on aquatic
 378 ecosystems and interactions with climate change, *Photochemical & Photobiological Sciences*, 10,
 379 242-260, 2011.
- 380 Halac, S. R., Villafane, V. E., Goncalves, R. J., and Helbling, E. W.: Photochemical responses of
 381 three marine phytoplankton species exposed to ultraviolet radiation and increased temperature: Role
 382 of photoprotective mechanisms, *Journal of Photochemistry and Photobiology B-Biology*, 141, 217-
 383 227, 10.1016/j.jphotobiol.2014.09.022, 2014.
- 384 Havaux, M., and Tardy, F.: Temperature-dependent adjustment of the thermal stability of
 385 photosystem II in vivo: Possible involvement of xanthophyll-cycle pigments, *Planta*, 198, 324-333,
 386 10.1007/bf00620047, 1996.



- 387 Helbling, E. W., Chalker, B. E., Dunlap, W. C., HolmHansen, O., and Villafane, V. E.:
388 Photoacclimation of Antarctic marine diatoms to solar ultraviolet radiation, *Journal of Experimental*
389 *Marine Biology and Ecology*, 204, 85-101, 10.1016/0022-0981(96)02591-9, 1996.
- 390 Heraud, P., and Beardall, J.: Changes in chlorophyll fluorescence during exposure of *Dunaliella*
391 *tertiolecta* to UV radiation indicate a dynamic interaction between damage and repair processes,
392 *Photosynthesis Research*, 63, 123-134, 10.1023/a:1006319802047, 2000.
- 393 Irwin, A. J., Nelles, A. M., and Finkel, Z. V.: Phytoplankton niches estimated from field data,
394 *Limnology and Oceanography*, 57, 787-797, 10.4319/lo.2012.57.3.0787, 2012.
- 395 Irwin, A. J., Finkel, Z. V., Mueller-Karger, F. E., and Ghinaglia, L. T.: Phytoplankton adapt to
396 changing ocean environments, *Proceedings of the National Academy of Sciences of the United*
397 *States of America*, 112, 5762-5766, 10.1073/pnas.1414752112, 2015.
- 398 Keithan, E. D., Lowe, R. L., and DeYoe, H. R.: Benthic diatom distribution in a pennsylvania stream:
399 role of pH and nutrients, *Journal of Phycology*, 24, 581-585, 1988.
- 400 Lavaud, J., Strzepak, R. F., and Kroth, P. G.: Photoprotection capacity differs among diatoms:
401 Possible consequences on the spatial distribution of diatoms related to fluctuations in the underwater
402 light climate, *Limnology and Oceanography*, 52, 1188-1194, 2007.
- 403 Lavaud, J., Six, C., and Campbell, D. A.: Photosystem II repair in marine diatoms with contrasting
404 photophysiologicals, *Photosynthesis Research*, 127, 189-199, 10.1007/s11120-015-0172-3, 2016.
- 405 Laviale, M., Barnett, A., Ezequiel, J., Lepetit, B., Frankenbach, S., Meleder, V., Serodio, J., and
406 Lavaud, J.: Response of intertidal benthic microalgal biofilms to a coupled light-temperature stress:
407 evidence for latitudinal adaptation along the Atlantic coast of Southern Europe, *Environmental*
408 *Microbiology*, 17, 3662-3677, 10.1111/1462-2920.12728, 2015.
- 409 Lavoie, M., Raven, J. A., and Levasseur, M.: Energy cost and putative benefits of cellular
410 mechanisms modulating buoyancy in aflagellate marine phytoplankton, *Journal of Phycology*, 52,
411 239-251, 10.1111/jpy.12390, 2016.
- 412 Levasseur, M., Therriault, J.-C., and Legendre, L.: Hierarchical control of phytoplankton succession
413 by physical factors, *Marine Ecology Progress Series*, 19, 211-222, 1984.
- 414 Melis, A.: Photosystem-II damage and repair cycle in chloroplasts: what modulates the rate of
415 photodamage in vivo?, *Trends in Plant Science*, 4, 130-135, 10.1016/s1360-1385(99)01387-4, 1999.
- 416 Morel, F. M. M., Rueter, J. G., Anderson, D. M., and Guillard, R. R. L.: Aquil: a chemically defined
417 phytoplankton culture medium for trace metal studies, *Journal of Phycology*, 15, 135-141,
418 10.1111/j.1529-8817.1979.tb02976.x, 1979.
- 419 Mosby, A. F., and Smith, W. O., Jr.: Phytoplankton growth rates in the Ross Sea, Antarctica, *Aquatic*
420 *Microbial Ecology*, 74, 157-171, 10.3354/ame01733, 2015.
- 421 New, M., Liverman, D., Schroeder, H., and Anderson, K.: Four degrees and beyond: the potential
422 for a global temperature increase of four degrees and its implications (vol 369, pg 6, 2011),
423 *Philosophical Transactions of the Royal Society a-Mathematical Physical and Engineering Sciences*,
424 369, 1112-1112, 10.1098/rsta.2010.0351, 2011.
- 425 Nitta, K., Suzuki, N., Honma, D., Kaneko, Y., and Nakamoto, H.: Ultrastructural stability under
426 high temperature or intensive light stress conferred by a small heat shock protein in cyanobacteria,
427 *Febs Letters*, 579, 1235-1242, 10.1016/j.febslet.2004.12.095, 2005.
- 428 Padfield, D., Yvon-Durocher, G., Buckling, A., Jennings, S., and Yvon-Durocher, G.: Rapid
429 evolution of metabolic traits explains thermal adaptation in phytoplankton, *Ecology Letters*, 19,
430 133-142, 10.1111/ele.12545, 2016.



- 431 Round, F. E., Crawford, R. M., and Mann, D. G.: Diatoms: Biology and Morphology of the Genera,
432 Cambridge University Press, 1990.
- 433 Souffreau, C., Vanormelingen, P., Verleyen, E., Sabbe, K., and Vyverman, W.: Tolerance of benthic
434 diatoms from temperate aquatic and terrestrial habitats to experimental desiccation and temperature
435 stress, *Phycologia*, 49, 309-324, 10.2216/09-30.1, 2010.
- 436 Stevenson, R. J.: Effects of Current and Conditions Simulating Autogenically Changing
437 Microhabitats on Benthic Diatom Immigration, *Ecology*, 64, 1514-1524, 10.2307/1937506, 1983.
- 438 Tedetti, M., and Sempere, R.: Penetration of ultraviolet radiation in the marine environment. A
439 review, *Photochemistry and Photobiology*, 82, 389-397, 10.1562/2005-11-09-ir-733, 2006.
- 440 Thomas, M. K., Kremer, C. T., Klausmeier, C. A., and Litchman, E.: A Global Pattern of Thermal
441 Adaptation in Marine Phytoplankton, *Science*, 338, 1085-1088, 10.1126/science.1224836, 2012.
- 442 Villareal, T. A.: Positive buoyancy in the oceanic diatom *Rhizosolenia debaryana* H. Peragallo, *Deep
443 Sea Research Part A. Oceanographic Research Papers*, 35, 1037-1045,
444 [http://dx.doi.org/10.1016/0198-0149\(88\)90075-1](http://dx.doi.org/10.1016/0198-0149(88)90075-1), 1988.
- 445 Weisse, T., Groeschl, B., and Bergkemper, V.: Phytoplankton response to short-term temperature
446 and nutrient changes, *Limnologia*, 59, 78-89, 10.1016/j.limno.2016.05.002, 2016.
- 447 Williamson, C. E., Zepp, R. G., Lucas, R. M., Madronich, S., Austin, A. T., Ballare, C. L., Norval,
448 M., Sulzberger, B., Bais, A. F., McKenzie, R. L., Robinson, S. A., Haeder, D.-P., Paul, N. D., and
449 Bormann, J. F.: Solar ultraviolet radiation in a changing climate, *Nature Climate Change*, 4, 434-
450 441, 10.1038/nclimate2225, 2014.
- 451 Wong, C.-Y., Teoh, M.-L., Phang, S.-M., Lim, P.-E., and Beardall, J.: Interactive Effects of
452 Temperature and UV Radiation on Photosynthesis of *Chlorella* Strains from Polar, Temperate and
453 Tropical Environments: Differential Impacts on Damage and Repair, *Plos One*, 10,
454 10.1371/journal.pone.0139469, 2015.
- 455 Wu, Y., Gao, K., Li, G., and Walter Helbling, E.: Seasonal impacts of solar UV radiation on
456 photosynthesis of phytoplankton assemblages in the coastal waters of the South China Sea,
457 *Photochemistry and Photobiology*, 86, 586-592, 10.1111/j.1751-1097.2009.00694.x, 2010.
- 458 Wu, Y., Li, Z., Du, W., and Gao, K.: Physiological response of marine centric diatoms to ultraviolet
459 radiation, with special reference to cell size, *Journal of Photochemistry and Photobiology B-Biology*,
460 153, 1-6, 10.1016/j.jphotobiol.2015.08.035, 2015.
- 461 Xie, S.-P., Deser, C., Vecchi, G. A., Ma, J., Teng, H., and Wittenberg, A. T.: Global Warming Pattern
462 Formation: Sea Surface Temperature and Rainfall, *Journal of Climate*, 23, 966-986,
463 10.1175/2009jcli3329.1, 2010.
- 464 Zudaire, L., and Roy, S.: Photoprotection and long-term acclimation to UV radiation in the marine
465 diatom *Thalassiosira weissflogii*, *Journal of Photochemistry and Photobiology B-Biology*, 62, 26-
466 34, 10.1016/s1011-1344(01)00150-6, 2001.
- 467



468 **Fig legends:**

469 Fig 1 The specific growth rates of both species under different temperature levels, vertical lines
470 represent SD, n=3.

471 Fig 2 The absorption spectra of methanol extracts of *Skeletonema sp.* and *Nitzschia sp.* cultured
472 under different temperature, spectra were normalized with value set as 1.0 at wavelength of 665nm,
473 vertical lines represent SD, n=3.

474 Fig 3 The quantum yields of 15 °C grown *Skeletonema sp.* and *Nitzschia sp.* under P or P+UVR for
475 1 hour exposure and subsequent recovery under dim light (gray area) for 1 hour, that were incubated
476 and measured at 15 °C (A: *Skeletonema sp.*, C: *Nitzschia sp.*) or 25 °C (B: *Skeletonema sp.*, D:
477 *Nitzschia sp.*), vertical lines represent SD, n=3.

478 Fig 4 The quantum yields of 20 °C grown *Skeletonema sp.* and *Nitzschia sp.* under P or P+UVR for
479 1 hour exposure and subsequent recovery under dim light (gray area) for 1 hour, that were incubated
480 and measured at 20 °C (A: *Skeletonema sp.*, C: *Nitzschia sp.*) or 30 °C (B: *Skeletonema sp.*, D:
481 *Nitzschia sp.*), vertical lines represent SD, n=3.

482 Fig 5 The quantum yields of 25 °C grown *Skeletonema sp.* and *Nitzschia sp.* under P or P+UVR for
483 1 hour exposure and subsequent recovery under dim light (gray area) for 1 hour, that were incubated
484 and measured at 25 °C (A: *Skeletonema sp.*, C: *Nitzschia sp.*) or 35 °C (B: *Skeletonema sp.*, D:
485 *Nitzschia sp.*), vertical lines represent SD, n=3.

486 Fig 6 The relative inhibition induced by UVR on the photosystem II of *Skeletonema sp.* (A) and
487 *Nitzschia sp.* (B) under grown or short term elevated temperature, vertical lines represent SD, n=3.

488 Fig 7 The repair rate (A) and damage rate (B) of photosystem II in *Skeletonema sp.* during P or
489 P+UVR exposure under grown temperature (acclimated) or short term elevated temperature
490 (short_term), and the ratio of repair to damage rate (C), vertical lines represent SD, n=3.

491 Fig 8 The repair rate (A) and damage rate (B) of photosystem II in *Nitzschia sp.* during P or P+UVR
492 exposure under grown temperature (acclimated) or short term elevated temperature(short_term),
493 and the ratio of repair to damage rate (C), vertical lines represent SD, n=3.

494

495 Fig 9 The rate constants for recovery of P exposed *Skeletonema sp.* (A) and *Nitzschia sp.* (B), and
496 rate constants for recovery of PAB exposed *Skeletonema sp.* (C) and *Nitzschia sp.* (D) under dim



497 light, samples were incubated under grown temperature (acclimated) or short term elevated
498 temperature (short_term), vertical lines represent SD, n=3.

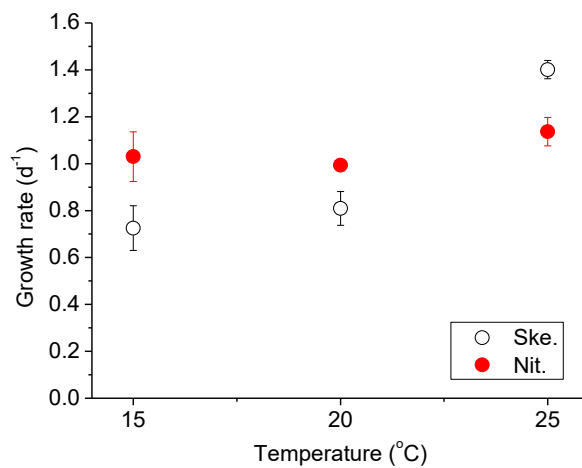


Fig 1

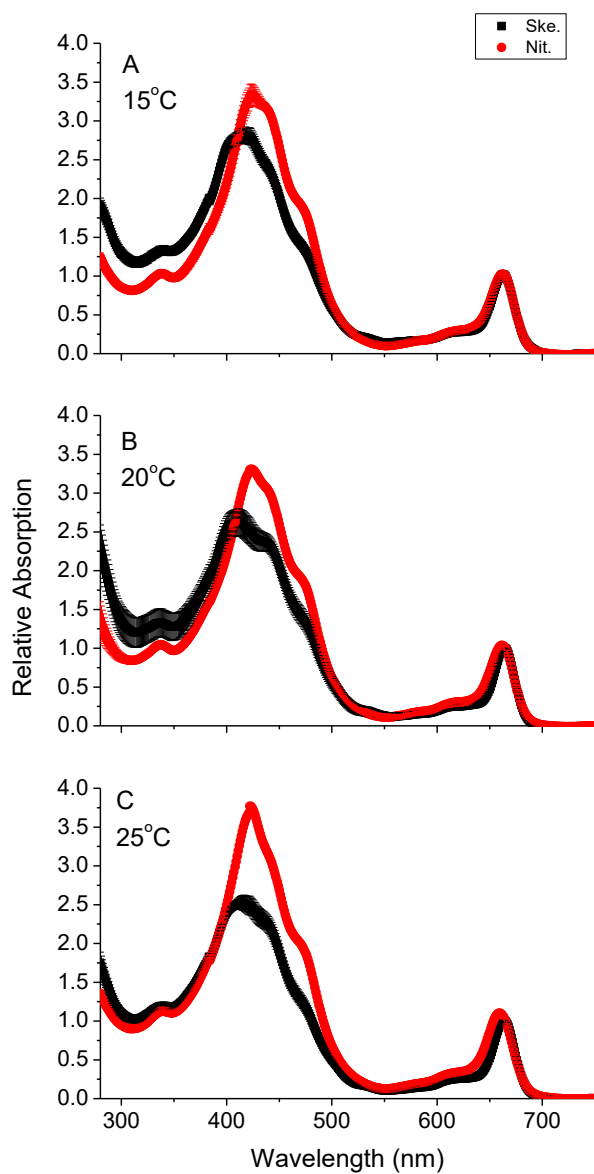


Fig 2

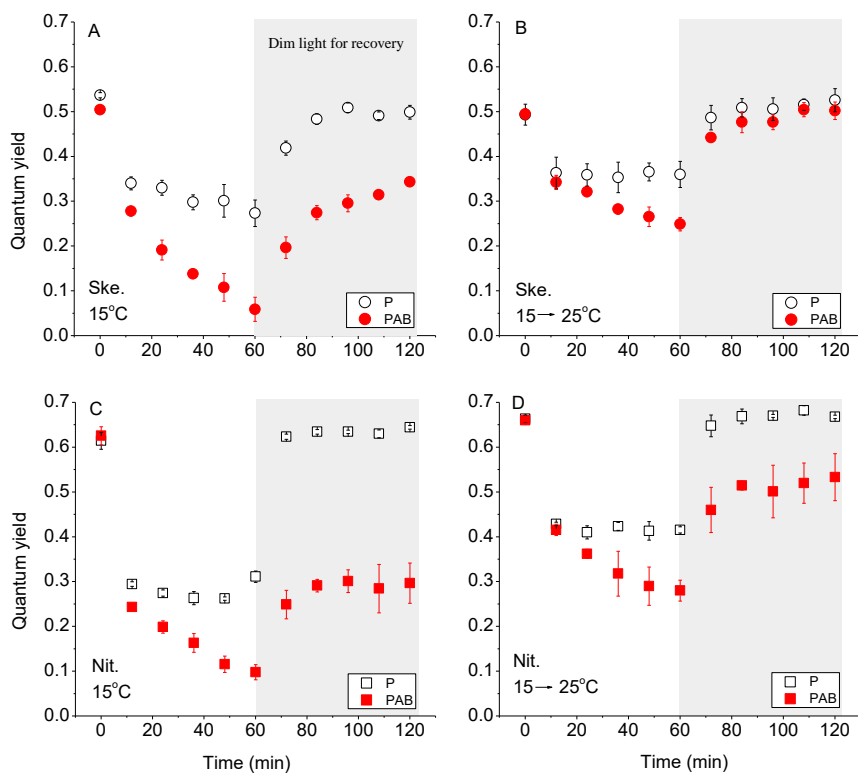


Fig 3

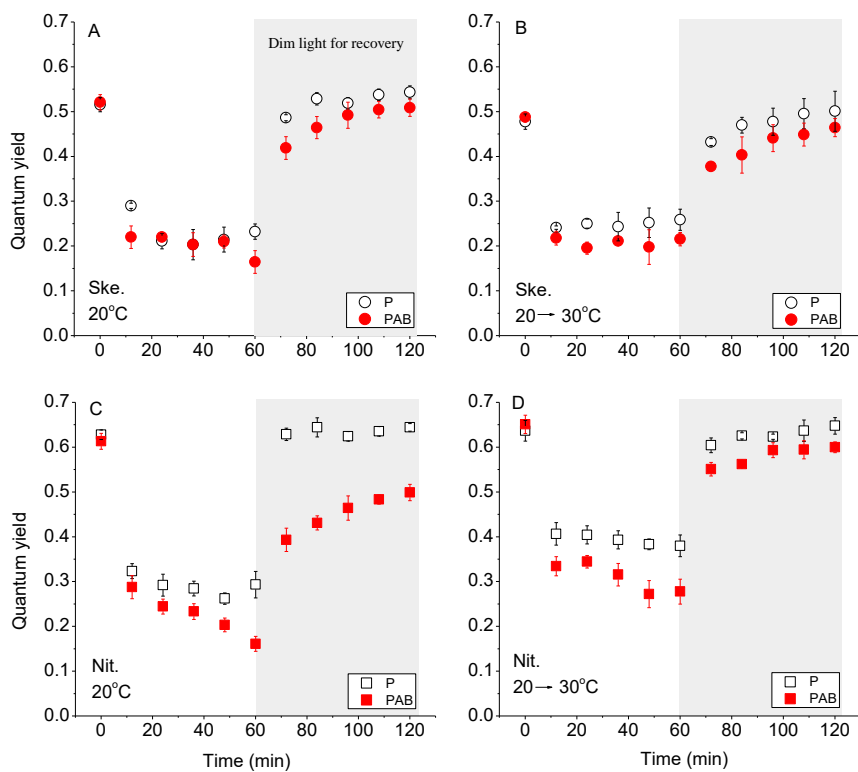


Fig 4

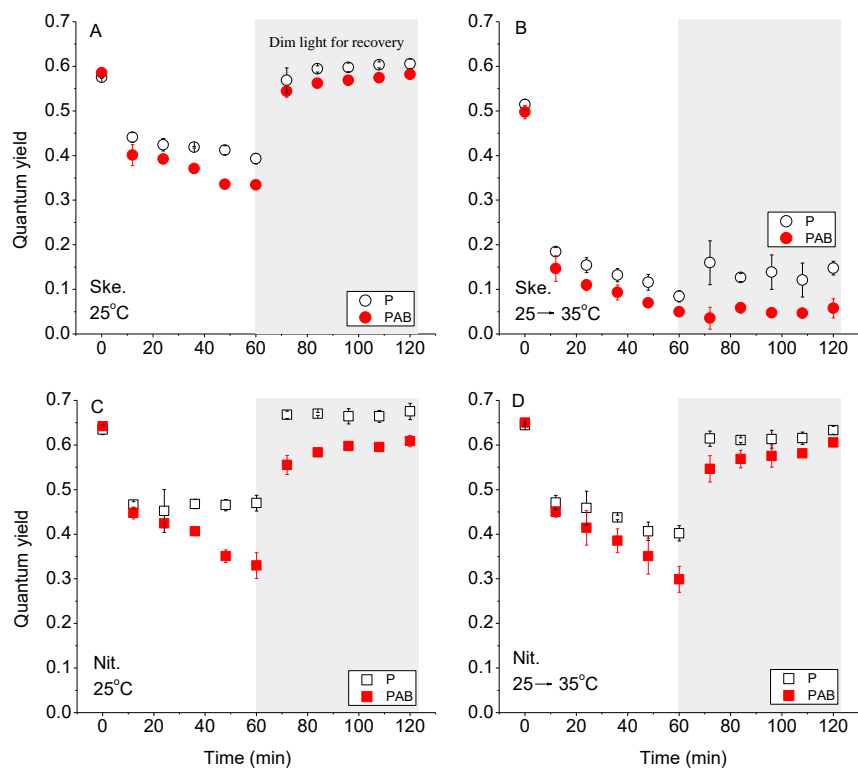


Fig 5

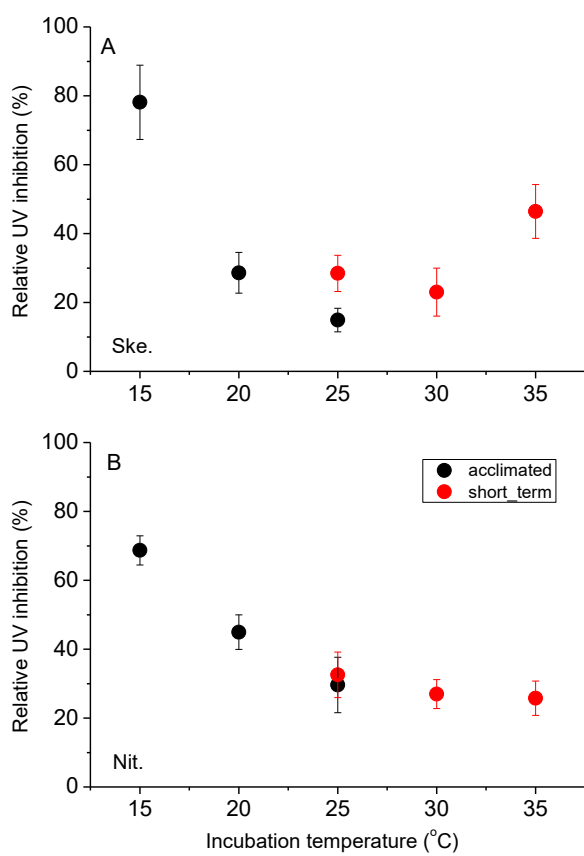


Fig 6

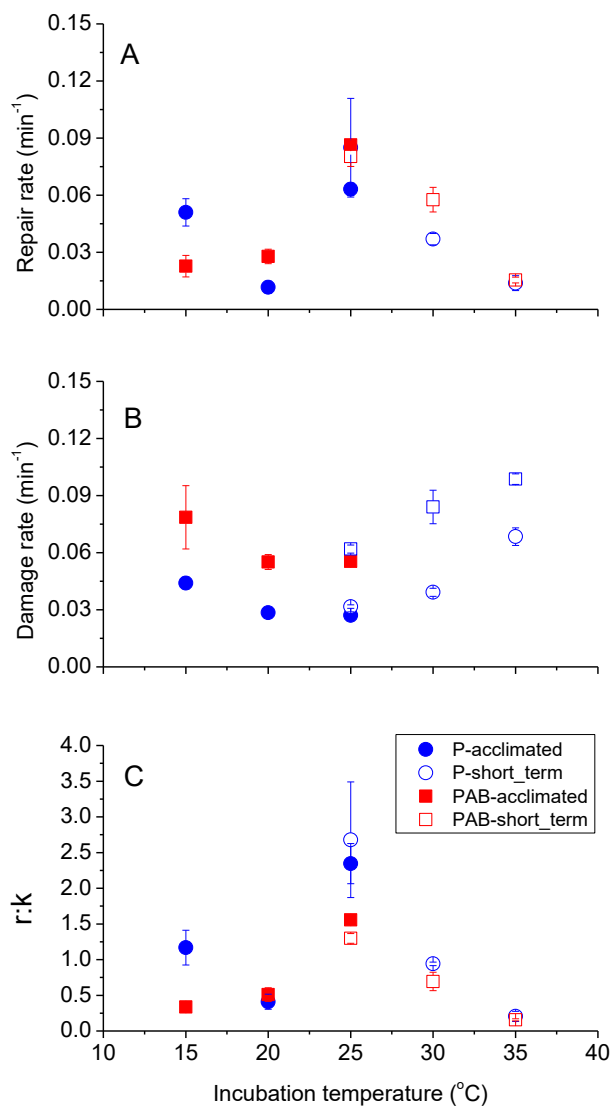


Fig 7

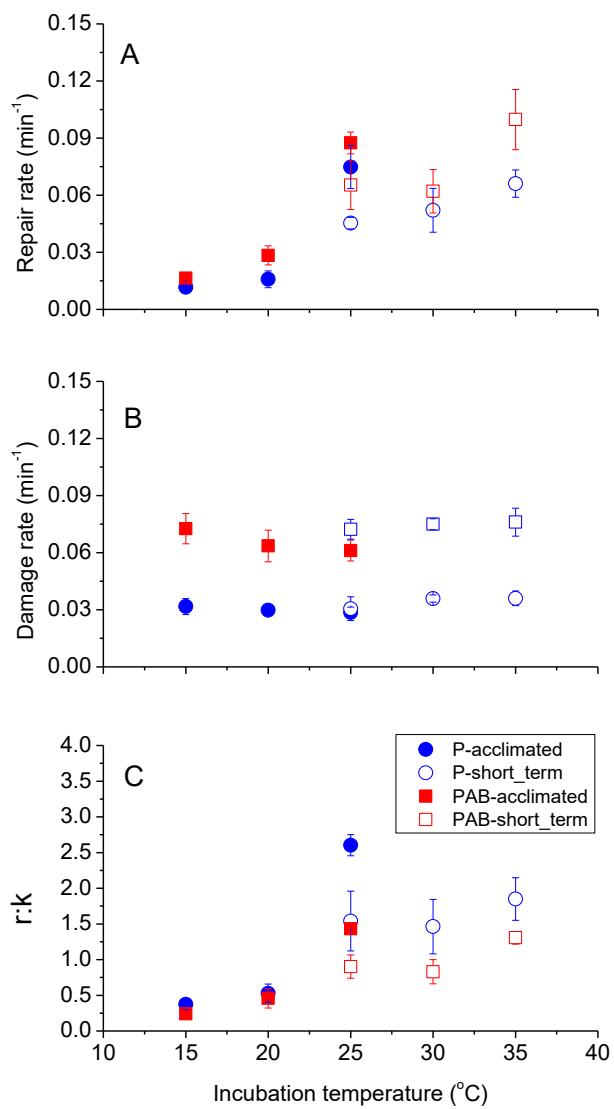


Fig 8

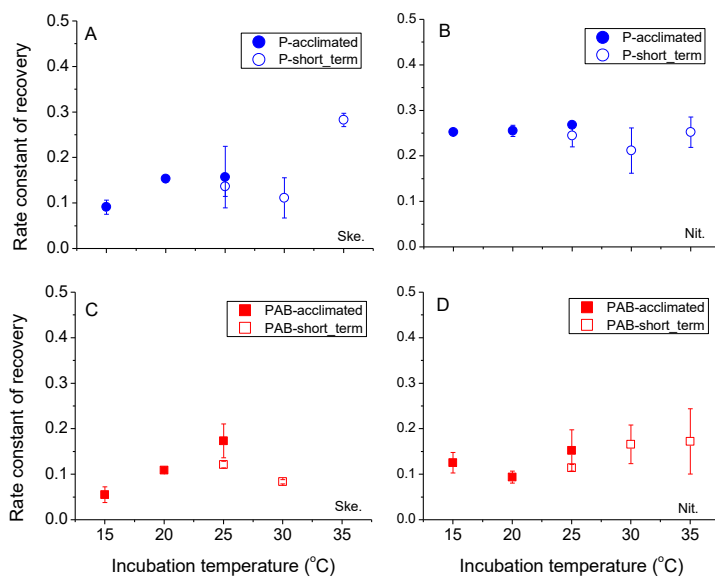


Fig 9

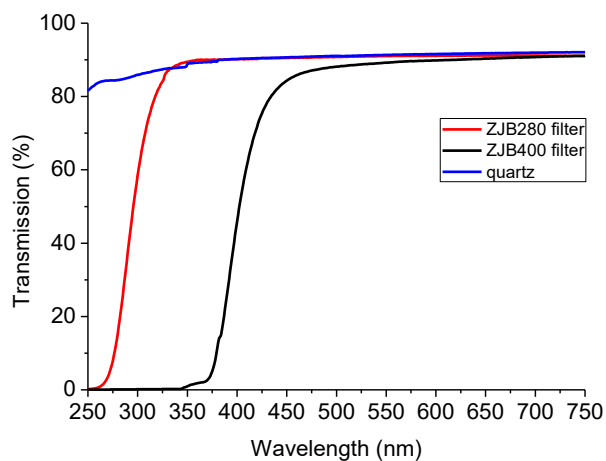


Figure A1 The transmission spectra (in percentage) of different cut-off filters (ZJB280, ZJB400) and the quartz tube between 280 and 750 nm.

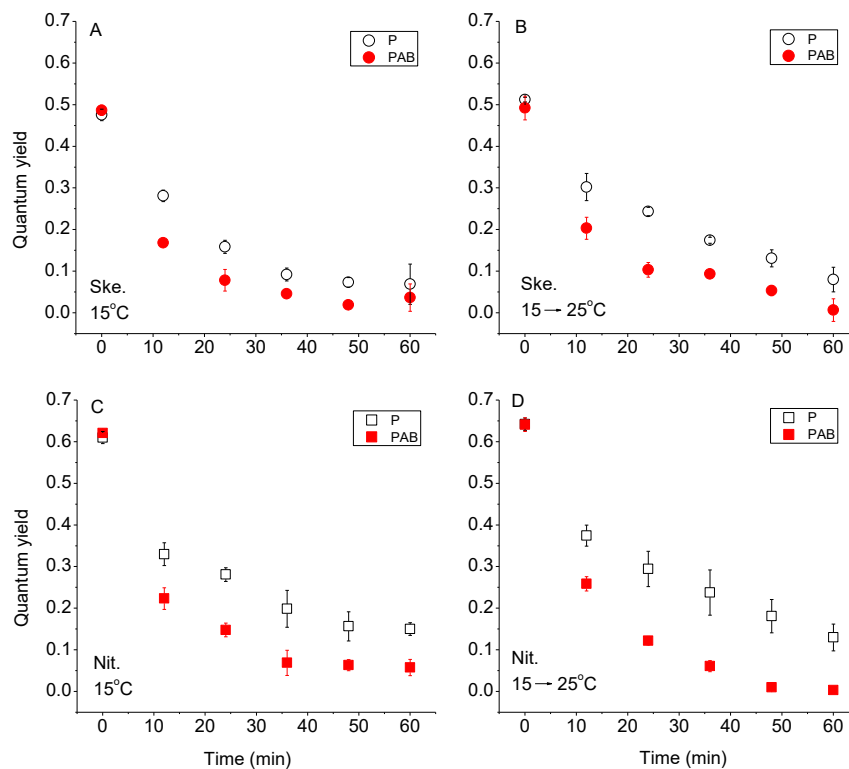


Figure A2 The quantum yields of 15 °C grown *Skeletonema sp.* and *Nitzschia sp.* under P or P+UVR for 1 hour exposure in the presence of lincomycin, that were incubated and measured at 15 °C (A, C) or 25 °C (B, D) , vertical lines represent SD, n=3.

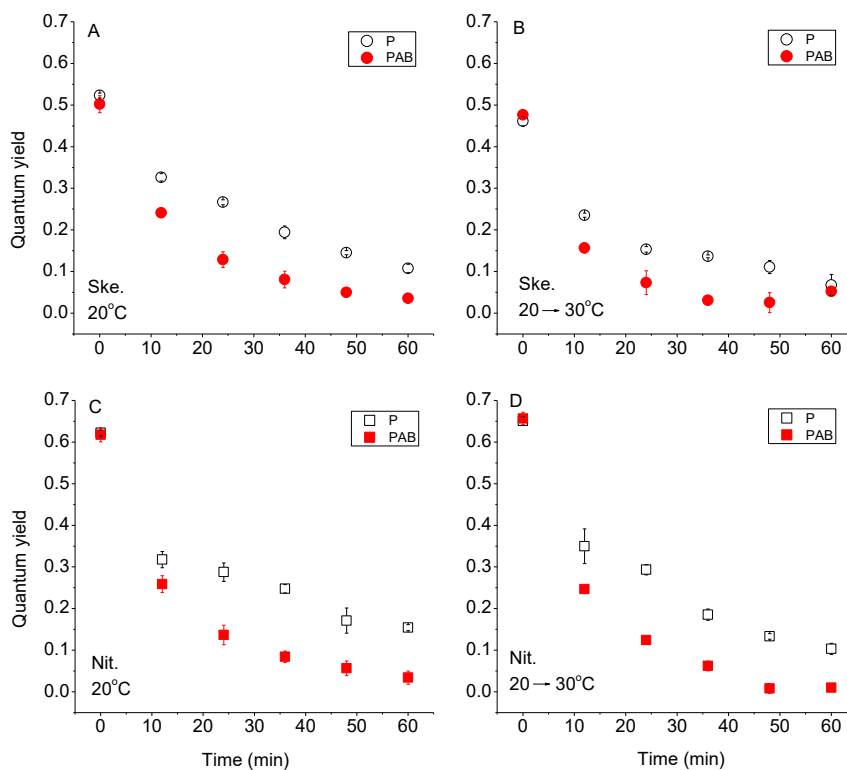


Figure A3 The quantum yields of 20 °C grown *Skeletonema sp.* and *Nitzschia sp.* under P or P+UVR for 1 hour exposure in the presence of lincomycin, that were incubated and measured at 20 °C (A, C) or 30 °C (B, D) , vertical lines represent SD, n=3.

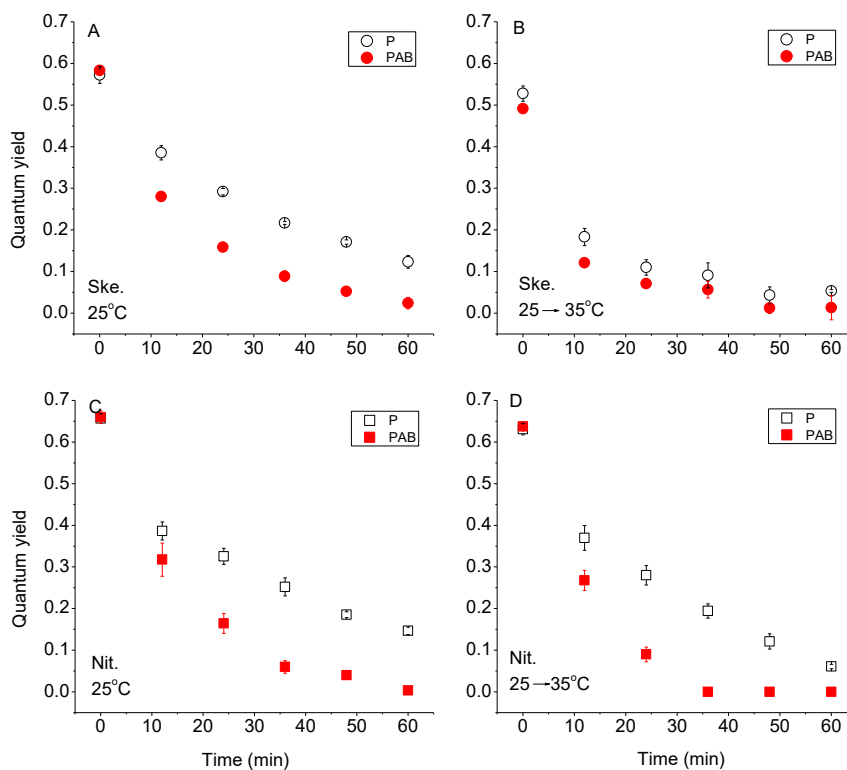


Figure A4 The quantum yields of 25 °C grown *Skeletonema sp.* and *Nitzschia sp.* under P or P+UVR for 1 hour exposure in the presence of lincomycin, that were incubated and measured at 25 °C (A, C) or 35 °C (B, D) , vertical lines represent SD, n=3.